PROCEEDINGS OF SCIENCE

Probing $g \to b\bar{b}$ with inclusive jets and V+jets with ATLAS

Valentina Maria Martina Cairo*, **on behalf of the ATLAS Collaboration**
SLAC National Accelerator Laboratory, CA - USA
E-mail: valentina.maria.cairo@cern.ch; vcairo@slac.stanford.edu

In this contribution, measurements performed by the ATLAS Collaboration at the Large Hadron Collider based on events containing jets or vector bosons plus jets aimed at probing gluon splitting will be summarised.

ATL-PHYS-PROC-2019-160
26 November 2019

7th Annual Conference on Large Hadron Collider Physics - LHCP2019
20-25 May, 2019
Puebla, Mexico

*Speaker.

PoS(LHCP2019)210

1. Introduction

Different production mechanisms can lead to the production of two jets from b-quarks. The lowest-order Feynman diagrams for $b\bar{b}$ production are shown in Figure 1. In flavour creation, both b-jets originate from the hard scatter: these jets tend to be the hardest in the event and are predicted to have an approximately back-to-back configuration in the transverse plane. The gluon splitting production mechanism creates a pair of b-jets that are expected to have a small angular separation. The topology of flavour excitation is less distinctive, but it tends to contain an additional parton, which reduces the angular separation between the b-jets. The dominant mechanism to

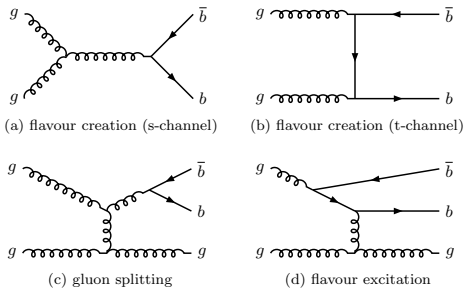

Figure 1: Lowest-order Feynman diagrams for $b\bar{b}$ production. Ref. [1]

produce two b-hadrons in one jet, typically in the high p_{T} regime, is the gluon splitting process $g \to b\bar{b}$. Gluon splitting shall be studied as a useful probe of perturbative Quantum Chromodynamics (pQCD): heavy flavours in initial states are qualitatively well understood to arise perturbatively from gluon splitting to b and c quarks, but there is an ambiguity between the two schemes which are generally employed in pQCD calculations containing heavy flavour quarks. One is the four-flavour number scheme (4FNS), which only considers parton densities of gluons and of the first two quark generations in the proton. The other is the five-flavour number scheme (5FNS), which allows a b-quark density in the initial state and raises the prospect that measurements of heavy flavour production could constrain the b-quark parton density function (PDF) of the proton. In a calculation to all orders, the 4FNS and 5FNS methods must give identical results; however, at a given order differences can occur between the two. A recent discussion on the status of theoretical calculations and the advantages and disadvantages of the different flavour number schemes can be found in Ref. [2].

Studying gluon splitting is fundamental not only as a pQCD probe, but also to understand the background composition and to control the related systematic uncertainties of many of the measurements of the Large Hadron Collider (LHC) physics programme. In fact, uncertainties related to gluon splitting constitute the leading systematic limitation on the sensitivity of the Higgs boson decaying to $b\bar{b}$ in ttH, VH and gluon fusion production modes. In particular, in boosted Higgs boson measurements, in which the angle between the 2 b-jets scales as the ratio between the mass and the momentum of the Higgs boson, studying $g \to b\bar{b}$ at small opening angle is of paramount importance.

Furthermore, events containing b-jets from gluon splitting constitute a background to many other SM measurements and searches by providing a source of additional real b-quark jets that can fake a signal for b-quarks originating from other processes.

In this contribution, measurements investigating gluon splitting as performed with the ATLAS Experiment [3] will be summarised. In Section 2 a quick recap of analyses based on events containing two b-jets or a Z boson plus b-jets will be given, while in Section 3 a dedicated measurement focusing on gluon splitting at small opening angles will be described.

2. Gluon splitting in Z+b-jets and $b\bar{b}$ dijets measurements

The ATLAS Collaboration has performed two measurements of vector boson plus b-jets at 7 TeV. One of them targets a W boson produced in association with b-jets [4], the other aims at measuring the differential production cross-section of a Z-boson in association with b-jets [5] as a function of several kinematic variables including the transverse momentum of the b-jet, the opening angle ΔR_{bb} between the two b-jets and the mass of the two b-jets m_{bb}, as shown in Figure 2. The theoretical predictions generally provide a good description of the shape of the measured cross-section as a function of the b-jet p_{T} as can be seen in Figure 2(a). When measuring the cross-section for the Z plus 2 b-jets category instead, all predictions still provide reasonable descriptions of the data within the large experimental uncertainties, but there is some evidence for disagreements between predictions and data at low m_{bb}, as clearly visible in Figure 2(b) and at low ΔR_{bb}, as visible in 2(c), where events produced via gluon splitting are concentrated. Thus, more investigation is needed at small ΔR_{bb}.

In fact, large differences between various Monte Carlo generator predictions were observed in this regime also in a simulation-only study performed at 13 TeV by the ATLAS Collaboration [6]. Figure 3 shows clear differences in the predictions of the various event generators when focusing on the small ΔR_{bb} region both for the events containing Z-bosons (Figure 3(a)) and for the events containing W-bosons (Figure 3(b)).

This regime was also investigated by measuring the differential di-b-jet production cross section at 7 TeV [1]. In particular, the differential cross-section as a function of ΔR_{bb} is shown in Figure 4, which still exhibits discrepancies between data and simulation at small values of ΔR_{bb}.

3. Gluon splitting at small opening angles

From the summary above, it is clear that the fragmentation of high-energy gluons at small opening angles is largely unconstrained by present measurements. Results using 7 TeV data showed a mismodeling of the small ΔR_{bb} region and motivated further investigation of $g \to b\bar{b}$ at small opening angle based on a 13 TeV data-set. Gluon splitting to b-quark pairs is a unique probe of the properties of gluon fragmentation because identified b-tagged jets provide a proxy for the quark daughters of the initial gluon. The key differential distributions of the $g \to b\bar{b}$ process were measured by ATLAS in 13 TeV data [17]. The high transverse momentum and low angular separation regime for $g \to b\bar{b}$ can be probed at the LHC by using b-tagged small-radius jets within large-radius jets. This topology is used to calibrate b-tagging in dense environments and is studied phenomenologically [18, 19]. Small-radius jets built from charged-particle tracks are used as proxies for b-quarks and can be exploited as precision probes of the small opening-angle regime.

All the details on the analysis strategy can be found in Ref. [17]. Below, the most important points are summarised.

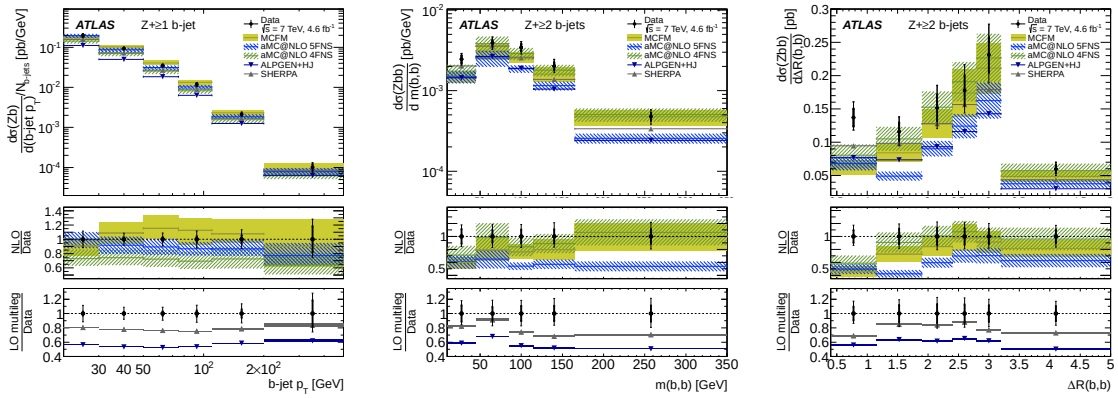

(a) (b) (c)

Figure 2: The inclusive b-jet cross-section $\sigma(Zb)\times$ the number of b-jets as a function of b-jet p_{T} 2(a). The cross-section $\sigma(Zbb)$ as a function of m_{bb} 2(b) and ΔR_{bb} 2(c). The top panels show measured differential cross-sections as filled circles with statistical (inner) and total (outer bar) uncertainties. Overlayed for comparison are the NLO predictions from MCFM [7] and aMC@NLO [8] both using the MSTW2008 [9] PDF set. The shaded bands represents the total theoretical uncertainty for MCFM and the uncertainty bands on aMC@NLO points represent the dominant theoretical scale uncertainty only. Also overlaid are LO multi-legged predictions for ALPGEN [10]+HERWIG [11] +JIMMY [12] and SHERPA [13]. The middle panels show the ratio of NLO predictions to data, and the lower panels show the ratio of LO predictions to data. Ref. [5].

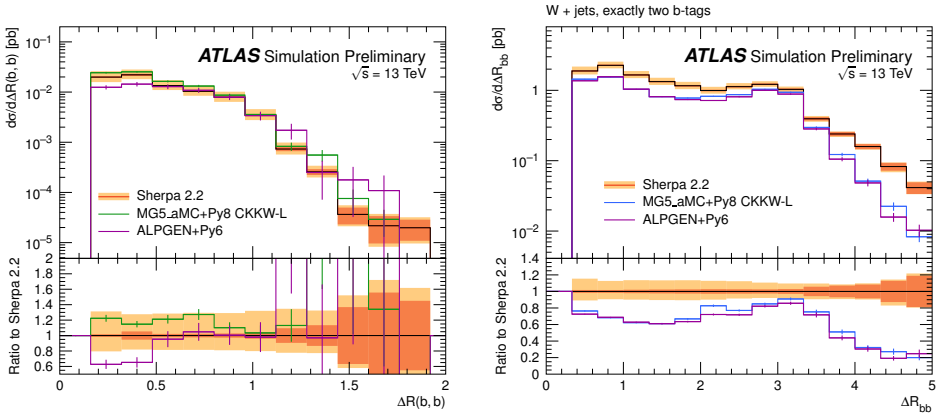

(a) (b)

Figure 3: Predictions for the differential cross sections as a function of the angular separation between the two b-tagged jets ΔR_{bb} in 3(a) Z-boson and 3(b) W-boson events from Sherpa 2.2 [13, 14], MG5_aMC@NLO [8] plus Pythia 8 using CKKW-L and ALPGEN [10]+Pythia 6 [15]. The orange band includes PDF and scale uncertainties estimated with Sherpa 2.2, while the size of the statistical uncertainty components are indicated by the size of the error bars. Ref. [6]

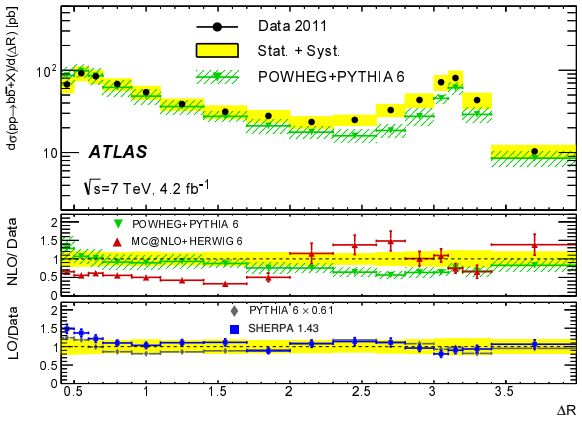

Figure 4: Top panel: the differential cross section for $b\bar{b}$ production as a function of the angular separation ΔR_{bb} between the two jets, compared to the theoretical predictions obtained using Powheg [16]. Theoretical uncertainties obtained by using Powheg are also shown. Middle panel: ratio of the NLO predictions to the measured cross section normalized to the same integrated luminosity. Bottom panel: ratio of the LO predictions to the measured cross section normalized to the same integrated luminosity. For the predictions from MC@NLO, SHERPA and Pythia 6 only the statistical uncertainties are shown. Ref. [1]

3.1 Event Selection

At detector level, events are selected using single-jet triggers requiring $p_{\mathrm{T}} > 450$ GeV and $|\eta| < 2$ and therefore these kinematic requirements are used to select jets for the measurement. The offline analysis requires the highest-p_{T} calorimeter jet to have at least two associated track-jets with $p_{\mathrm{T}} > 10$ GeV and $|\eta| < 2.5$. In order to enhance the $g \to b\bar{b}$ purity, the leading track-jet associated with the selected calorimeter jet must be b-tagged. Requiring both track-jets to be b-tagged increases the purity but would degrade the precision of the background fit and so only one is required. At particle level events are required to have at least one large-radius jet with $p_{\mathrm{T}} > 450$ GeV. The leading jet needs to have at least two associated particle-level track-jets[1] with $p_{\mathrm{T}} > 10$ GeV. Both of the associated small-radius jets must be tagged as b-jets. This inclusive event selection produces a sample where QCD scattering processes dominate.

3.2 Oservables

The kinematic properties of the $g \to b\bar{b}$ process are characterized by three quantities: the opening angle between the b-quarks ΔR_{bb}, the momentum sharing between the b-quarks $z(p_{\mathrm{T}}) = p_{\mathrm{T},2}/p_{\mathrm{T},1} + p_{\mathrm{T},2})$, where $p_{\mathrm{T},1}$ and $p_{\mathrm{T},2}$ are the transverse momenta of the leading and subleading track-jets, respectively, and the orientation of the gluon splitting relative to the gluon production plane $\Delta\theta_{ppg,gbb}$. The observable $\Delta\theta_{ppg,gbb}$ is defined as the angle between the plane spanned by the beam line and the vector sum of the two track-jets and the plane spanned by the two track-jets. In addition to these quantities, the dimensionless mass $\log(m_{bb}/p_{\mathrm{T}})$ is also measured, where the

[1] Particle-level jets are clustered using the same algorithms as for detector-level jets, except the inputs to jet finding are all stable particles ($c\tau > 10$ mm) excluding all muons and neutrinos. The same trimming algorithm applied to calorimeter jets is also applied to the large-radius particle-level jets. Particle-level track-jets are formed from all stable charged particles that have $p_{\mathrm{T}} > 500$ MeV and $|\eta| < 2.5$, excluding muons.

mass and transverse momentum in the logarithm are computed from the four-vector sum of the two track-jets.

3.3 Background and Systematic Uncertainties

After the event selection, the contribution from large-radius jets that do not have two associated track-jets containing b-hadrons is subtracted from data, before correcting for detector effects via unfolding. The fraction of background events may not be well modeled by the simulation, so correction factors are determined from data template fits to the impact parameter distribution and applied for each bin of the four target observables of the analysis prior to subtraction. Systematic and statistical uncertainties were assessed for each aspect of the analysis, including the background subtraction, acceptance and efficiency correction factors, response matrix, and unfolding method. For each uncertainty, a component of the analysis chain is varied and then the entire procedure including the background subtraction is repeated. The jet energy scale, the unfolding, and the theoretical modeling uncertainties dominate.

3.4 Results

The unfolded results along with multiple parton shower MC predictions are presented in Figure 5. The Sherpa [13] predictions are generally more accurate than those from Pythia 8 [20, 21], although there are significant differences between both generators and the data at low mass, low $z(p_{\mathrm{T}})$ and all values of $\Delta\theta_{ppg,gbb}$. The $\Delta\theta_{ppg,gbb}$ distribution in data appears to be inverted with respect to the one from Pythia 8 (with a minimum instead of maximum at $\pi/2$), while Sherpa predicts a relatively uniform distribution. In general, the properties of gluon polarization inside unpolarized hadrons are largely unconstrained by experimental data. This and future measurements of $\Delta\theta_{ppg,gbb}$ may provide a new way to extract p_{T}-dependent parton distributions in order to better understand proton structure and further improve the precision of various cross-section calculations. In addition to studying gluon production properties, $g \to b\bar{b}$ provides a handle on gluon fragmentation. Due to the large b-quark mass and in general the large m_{bb} mass that is possible after splitting, there are many formally equivalent model choices in describing gluon fragmentation. For example, the scale at which the strong coupling constant acts (renormalization scale) may be better described as scaling with m_{bb}^2 instead of the Pythia 8 default $p_{\mathrm{T},bb}^2$. To illustrate the sensitivity of the observables to fragmentation settings in Pythia 8, the plots in Figure 5 show the final-state radiation variations of the A14 tune (indicated as an uncertainty band in the plot) as well as a different way to treat the b-quark mass in the QCD splitting kernels indicated by the $m_{bb}^2/4$ variation. No variation describes all of the data, with some variations being worse than others. For example, the Var2+ A14 variation, which increases the final-state shower $\alpha_s(M_Z)$ value to 0.139, moves the prediction further from the data in nearly all measurement bins.

4. Conclusions

Studying $g \to b\bar{b}$ is of paramount importance both as a probe of pQCD and as a way to better understand the background events to $H \to b\bar{b}$ searches or measurements. The ATLAS Experiment at the LHC has studied $g \to b\bar{b}$ with b-jets and vector boson plus b-jets at 7 TeV. These results showed a mismodeling in the small angular region and motivated further investigation of $g \to b\bar{b}$

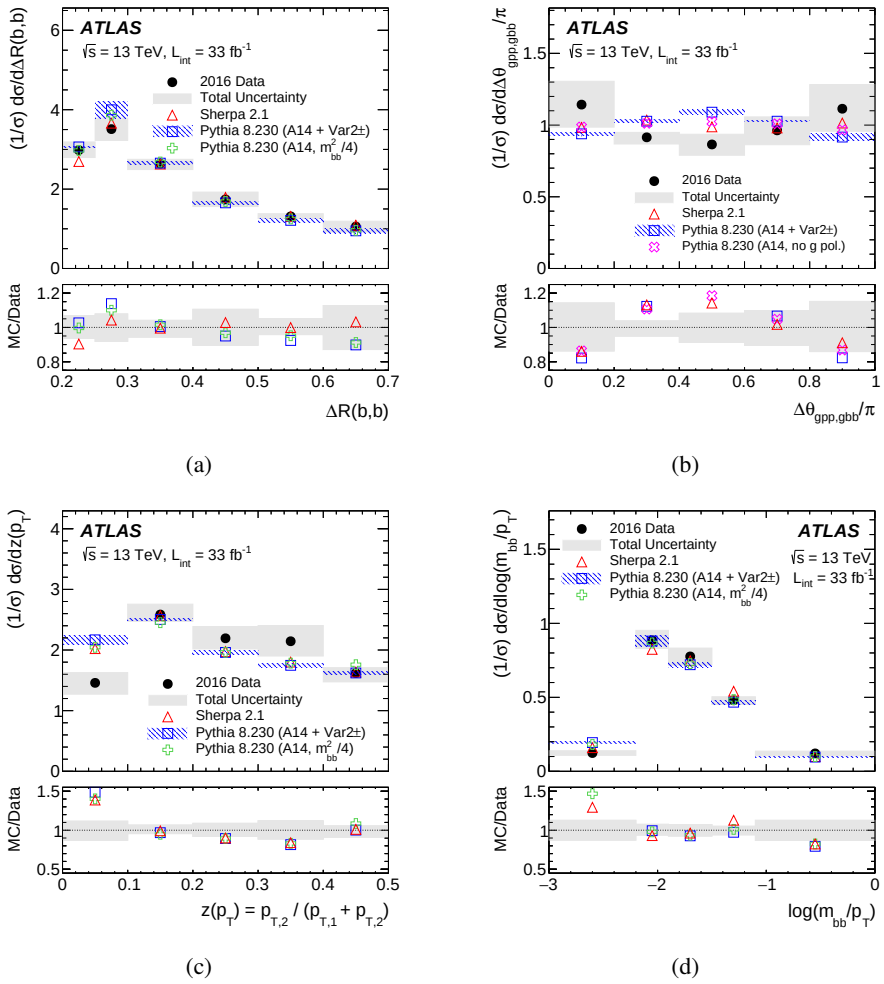

Figure 5: The unfolded distribution of 5(a) ΔR_{bb}, 5(b) $\Delta\theta_{ppg,gbb}$, 5(c) $z(p_{\mathrm{T}})$ and 5(d) and $\log(m_{bb}/p_{\mathrm{T}})$. Error bands represent the sum in quadrature of statistical and systematic uncertainties. These data are compared with predictions from the Pythia 8 and Sherpa MC simulations. The bands for the Pythia 8 prediction represented by a square indicate the Var2± variations (dominated by a ±10% variation in the final state shower α_s). The additional set of Pythia 8 markers use $m_{bb}^2/4$ for the renormalization scale. Ref. [17]

in this regime. A dedicated 13 TeV analysis was performed. Simulations from the Sherpa event generator generally provide a better model than Pythia 8, especially for the $\Delta\theta_{ppg,gbb}$ observable which is sensitive to the modeling of the gluon polarization. The particle-level spectra are publicly available for further interpretation and can be used to validate QCD MC predictions and tune their models' free parameters.

References

[1] ATLAS Collaboration. "Measurement of the $b\bar{b}$ dijet cross section in pp collisions at $\sqrt{s} =$ 7 TeV with the ATLAS detector". In: Eur. Phys. J. C 76 (2016), p. 670. DOI: 10.1140/epjc/s10052-016-4521-y. arXiv: 1607.08430 [hep-ex].

[2] Fabio Maltoni, Giovanni Ridolfi, and Maria Ubiali. "b-initiated processes at the LHC: a reappraisal". In: JHEP 2012.7 (2012), p. 22. ISSN: 1029-8479. DOI: 10.1007/JHEP07(2012)022. URL: https://doi.org/10.1007/JHEP07(2012)022.

[3] ATLAS Collaboration. "The ATLAS Experiment at the CERN Large Hadron Collider". In: JINST 3 (2008), S08003. DOI: 10.1088/1748-0221/3/08/S08003.

[4] ATLAS Collaboration. "Measurement of the cross-section for W boson production in association with b-jets in pp collisions at $\sqrt{s} = 7$ TeV with the ATLAS detector". In: JHEP 06 (2013), p. 084. DOI: 10.1007/JHEP06(2013)084. arXiv: 1302.2929 [hep-ex].

[5] The ATLAS collaboration. "Measurement of differential production cross-sections for a Z boson in association with b-jets in 7 TeV proton-proton collisions with the ATLAS detector". In: JHEP 2014.10 (2014), p. 141. ISSN: 1029-8479. DOI: 10.1007/JHEP10(2014)141. URL: https://doi.org/10.1007/JHEP10(2014)141.

[6] ATLAS Collaboration. "ATLAS simulation of boson plus jets processes in Run 2". ATL-PHYS-PUB-2017-006. 2017. URL: https://cds.cern.ch/record/2261937.

[7] John M. Campbell and R.K. Ellis. "MCFM for the Tevatron and the LHC". In: Nuclear Physics B - Proceedings Supplements 205-206 (2010), 10–15. ISSN: 0920-5632. DOI: 10.1016/j.nuclphysbps.2010.08.011. URL: http://dx.doi.org/10.1016/j.nuclphysbps.2010.08.011.

[8] J. Alwall et al. "The automated computation of tree-level and next-to-leading order differential cross sections, and their matching to parton shower simulations". In: JHEP 2014.7 (2014). ISSN: 1029-8479. DOI: 10.1007/jhep07(2014)079. URL: http://dx.doi.org/10.1007/JHEP07(2014)079.

[9] A. D. Martin et al. "Parton distributions for the LHC". In: Eur. Phys. J. C 63.2 (2009), 189–285. ISSN: 1434-6052. DOI: 10.1140/epjc/s10052-009-1072-5. URL: http://dx.doi.org/10.1140/epjc/s10052-009-1072-5.

[10] Michelangelo L Mangano et al. "ALPGEN, a generator for hard multiparton processes in hadronic collisions". In: JHEP 2003.07 (2003), 001–001. ISSN: 1029-8479. DOI: 10.1088/1126-6708/2003/07/001. URL: http://dx.doi.org/10.1088/1126-6708/2003/07/001.

[11] Gennaro Corcella et al. "HERWIG 6: an event generator for hadron emission reactions with interfering gluons (including supersymmetric processes)". In: JHEP 2001.01 (2001), 010–010. ISSN: 1029-8479. DOI: 10.1088/1126-6708/2001/01/010. URL: http://dx.doi.org/10.1088/1126-6708/2001/01/010.

[12] J. M. Butterworth, J. R. Forshaw, and M. H. Seymour. "Multiparton interactions in photoproduction at HERA". In: Zeitschrift für Physik C: Particles and Fields 72.4 (1996), 637–646. ISSN: 1431-5858. DOI: 10.1007/s002880050286. URL: http://dx.doi.org/10.1007/s002880050286.

[13] T Gleisberg et al. "Event generation with SHERPA 1.1". In: JHEP 2009.02 (2009), 007–007. ISSN: 1029-8479. DOI: 10.1088/1126-6708/2009/02/007. URL: http://dx.doi.org/10.1088/1126-6708/2009/02/007.

[14] Enrico Bothmann et al. “Event Generation with Sherpa 2.2”. In: SciPost Phys. 7 (3 2019), p. 34. DOI: 10.21468/SciPostPhys.7.3.034. URL: https://scipost.org/10.21468/SciPostPhys.7.3.034.

[15] Torbjörn Sjöstrand, Stephen Mrenna, and Peter Skands. “PYTHIA 6.4 physics and manual”. In: JHEP 2006.05 (2006), 026–026. ISSN: 1029-8479. DOI: 10.1088/1126-6708/2006/05/026. URL: http://dx.doi.org/10.1088/1126-6708/2006/05/026.

[16] Stefano Frixione, Paolo Nason, and Carlo Oleari. “Matching NLO QCD computations with parton shower simulations: the POWHEG method”. In: *Journal of High Energy Physics* 2007.11 (2007), pp. 070–070. DOI: 10.1088/1126-6708/2007/11/070. URL: https://doi.org/10.1088%2F1126-6708%2F2007%2F11%2F070.

[17] ATLAS Collaboration. “Properties of $g \to b\bar{b}$ at small opening angles in pp collisions with the ATLAS detector at $\sqrt{s} = 13$ TeV”. In: Phys. Rev. D 99 (2019), p. 052004. DOI: 10.1103/PhysRevD.99.052004. arXiv: 1812.09283 [hep-ex].

[18] ATLAS Collaboration. "Studies of b-tagging performance and jet substructure in a high p_T g→bb rich sample of large-R jets from pp collisions at $\sqrt{s} = 13$ TeV with the ATLAS detector". ATLAS-CONF-2016-002. 2016. URL: https://cds.cern.ch/record/2135187.

[19] ATLAS Collaboration. "Boosted Higgs ($\to b\bar{b}$) Boson Identification with the ATLAS Detector at $\sqrt{s} = 13$ TeV". ATLAS-CONF-2016-039. 2016. URL: https://cds.cern.ch/record/2206038.

[20] Peter Skands, Stefano Carrazza, and Juan Rojo. “Tuning PYTHIA 8.1: the Monash 2013 Tune”. In: Eur.Phys.J. C74.8 (2014), p. 3024.

[21] The ATLAS Collaboration. "Further ATLAS tunes of PYTHIA6 and Pythia 8". eprint: ATL-PHYS-PUB-2011-014.